# JCI The Journal of Clinical Investigation

# Autophagy influences glomerular disease susceptibility and maintains podocyte homeostasis in aging mice

Björn Hartleben, … , Gerd Walz, Tobias B. Huber

**Research Article**  **Nephrology**

Injury and loss of podocytes are leading factors of glomerular disease and renal failure. The postmitotic podocyte is the primary glomerular target for toxic, immune, metabolic, and oxidant stress, but little is known about how this cell type copes with stress. Recently, autophagy has been identified as a major pathway that delivers damaged proteins and organelles to lysosomes in order to maintain cellular homeostasis. Here we report that podocytes exhibit an unusually high level of constitutive autophagy. Podocyte-specific deletion of autophagy-related 5 (*Atg5*) led to a glomerulopathy in aging mice that was accompanied by an accumulation of oxidized and ubiquitinated proteins, ER stress, and proteinuria. These changes resulted ultimately in podocyte loss and late-onset glomerulosclerosis. Analysis of pathophysiological conditions indicated that autophagy was substantially increased in glomeruli from mice with induced proteinuria and in glomeruli from patients with acquired proteinuric diseases. Further, mice lacking Atg5 in podocytes exhibited strongly increased susceptibility to models of glomerular disease. These findings highlight the importance of induced autophagy as a key homeostatic mechanism to maintain podocyte integrity. We postulate that constitutive and induced autophagy is a major protective mechanism against podocyte aging and glomerular injury, representing a putative target to ameliorate human glomerular disease and aging-related loss of renal function.

**Find the latest version:**

https://jci.me/39492/pdf

# Autophagy influences glomerular disease susceptibility and maintains podocyte homeostasis in aging mice

Björn Hartleben,[1] Markus Gödel,[1,2] Catherine Meyer-Schwesinger,[3] Shuya Liu,[1] Theresa Ulrich,[1] Sven Köbler,[1] Thorsten Wiech,[4] Florian Grahammer,[1] Sebastian J. Arnold,[1] Maja T. Lindenmeyer,[5] Clemens D. Cohen,[5] Hermann Pavenstädt,[6] Dontscho Kerjaschki,[7] Noboru Mizushima,[8] Andrey S. Shaw,[9] Gerd Walz,[1,2] and Tobias B. Huber[1,2]

[1]Renal Division, University Hospital Freiburg, Germany. [2]Centre for Biological Signalling Studies (bioss), Albert-Ludwigs-Universität Freiburg, Germany. [3]Renal Unit, Department of Internal Medicine, University Hospital Hamburg-Eppendorf, Hamburg, Germany. [4]Department of Pathology, University Hospital Freiburg. [5]Division of Nephrology and Institute of Physiology, University Hospital and University of Zurich, Switzerland. [6]Renal Division, University Hospital Münster, Germany. [7]Department of Pathology, Medical University of Vienna, Austria. [8]Department of Physiology and Cell Biology, Tokyo Medical and Dental University, Japan. [9]Department of Pathology and Immunology, Washington University, St. Louis, Missouri.

**Injury and loss of podocytes are leading factors of glomerular disease and renal failure. The postmitotic podocyte is the primary glomerular target for toxic, immune, metabolic, and oxidant stress, but little is known about how this cell type copes with stress. Recently, autophagy has been identified as a major pathway that delivers damaged proteins and organelles to lysosomes in order to maintain cellular homeostasis. Here we report that podocytes exhibit an unusually high level of constitutive autophagy. Podocyte-specific deletion of autophagy-related 5 (*Atg5*) led to a glomerulopathy in aging mice that was accompanied by an accumulation of oxidized and ubiquitinated proteins, ER stress, and proteinuria. These changes resulted ultimately in podocyte loss and late-onset glomerulosclerosis. Analysis of pathophysiological conditions indicated that autophagy was substantially increased in glomeruli from mice with induced proteinuria and in glomeruli from patients with acquired proteinuric diseases. Further, mice lacking Atg5 in podocytes exhibited strongly increased susceptibility to models of glomerular disease. These findings highlight the importance of induced autophagy as a key homeostatic mechanism to maintain podocyte integrity. We postulate that constitutive and induced autophagy is a major protective mechanism against podocyte aging and glomerular injury, representing a putative target to ameliorate human glomerular disease and aging-related loss of renal function.**

## Introduction

The kidney filtration barrier is a unique structure characterized by a complex 3-dimensional framework of podocytes and endothelial cells. Podocytes form fine interdigitating foot processes, which envelope the glomerular capillaries (1, 2). In order to maintain the kidney filtration barrier, podocytes have to function as specific pericytes, counteracting the high transmural distending forces; serve as molecular sieves that establish the selective permeability properties of the glomerular filter; secrete soluble factors to regulate other cell types within the glomerulus; and coordinate dynamic signaling events at the slit diaphragm. The combination of all these functions in one cell is reflected by the high differentiation, the neuron-like appearance, and the very complex cytoarchitecture of podocytes. Unlike all other cell types forming the kidney filtration apparatus, podocytes have a very limited capacity for cell division and replacement (2). The fate of podocytes therefore entirely depends on their ability to cope with stress.

Recent research indicates that a decrease in the number of glomerular podocytes is a predictor for the progression of renal diseases, including focal segmental glomerulosclerosis and dia-betic nephropathy (3–5). In addition, increased appearance of podocytes and podocyte constituents in the urine is associated with glomerulosclerosis (6, 7). Together these data underline the concept that loss of podocytes triggers glomerulosclerosis. Furthermore, progressive glomerulosclerosis leads to an irreversible loss of renal function, ultimately culminating in end-stage renal disease (ESRD). Podocyte injury is therefore a key determinant of glomerular diseases and ESRD. Glomerulosclerosis in combination with loss of glomerular filtration also typically occurs in the aging human kidney. Animal models indicate that the age-dependent development of glomerulosclerosis is due to a loss of podocytes (8, 9). However, the mechanism by which this might occur has not been elucidated.
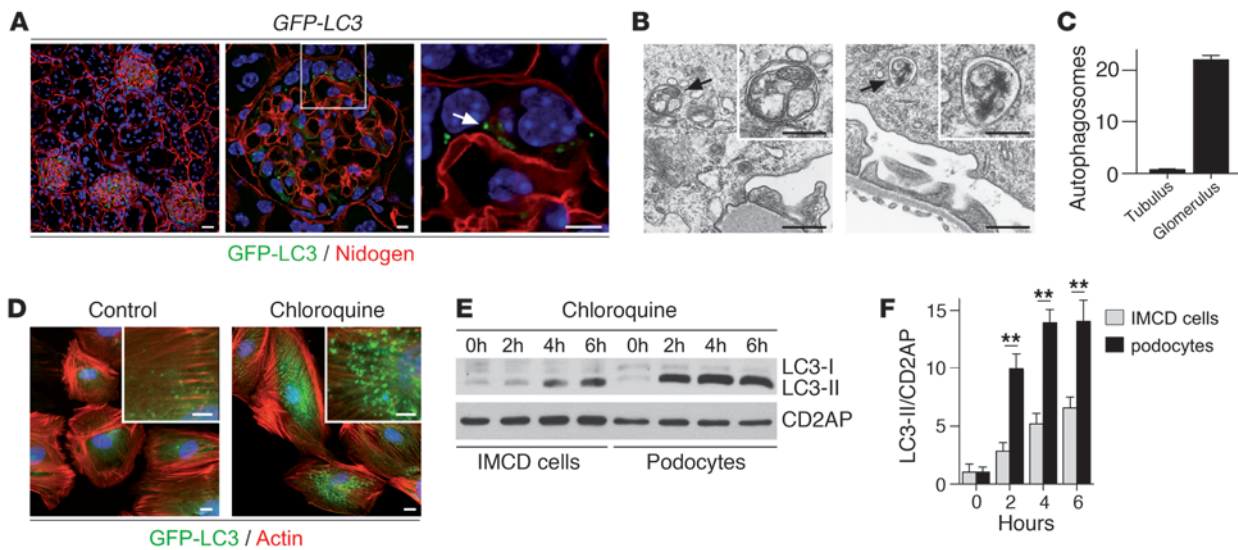
Increasing age causes a progressive deterioration of most tissues, leading to an impairment of cell function and increased vulnerability to environmental challenges. The accumulation of damaged proteins, lipids, and organelles usually accounts for the age-associated malfunctioning of individual cells (10). Recent studies have demonstrated that a decreased rate of protein degradation is responsible for the age-dependent functional decline in many cell types (10).

The 2 major protein degradation pathways in eukaryotes are the ubiquitin-proteasome system (UPS) and autophagy (11). Both of these systems are responsible for the efficient degradation and turnover of proteins within the cell. Failure of either

**Figure 1**
Glomerular podocytes exert high levels of autophagy under basal conditions. (**A**) In vivo analysis of autophagy using *GFP-LC3* transgenic mice (arrow indicates autophagosome within the podocyte; nidogen served as a marker for the basement membrane). (**B**) Autophagosome (arrow, left) and autolysosome (arrow, right) on electron micrographs in podocytes of wild-type mice. (**C**) Podocytes displayed high levels of autophagy under basal conditions compared with tubular cells (*n* = 3 *GFP-LC3* transgenic mice, 30 tubules and glomeruli of each mouse were analyzed). (**D**) Inhibition of autophagosomal degradation with chloroquine in differentiated podocytes induced a rapid accumulation of GFP-LC3–positive autophagosomes in *GFP-LC3*–transgenic podocytes. (**E** and **F**) Comparison of LC3-II accumulation in IMCD cells and differentiated podocytes in the presence of the lysosomal inhibitor chloroquine. CD2AP served as a loading control. Densitometric analysis indicated the significantly faster accumulation of LC3-II in differentiated podocytes (\*\**P* < 0.01, 2-tailed Student's *t* test; 3 independent experiments). Scale bars: 20 μm (**A**, left, and **D**), 5 μm (**A**, middle and right); 500 nm (**B**), 250 nm (**B**, insets); 10 μm (**D**, insets).

the UPS or autophagy has been associated with disease, while the upregulation of these processes has been shown to ameliorate certain disease entities (11, 12). The proteasome is responsible for the selective degradation or recycling of short-lived cytosolic proteins but also regulates the turnover of some long-lived proteins. Due to the size of the narrow barrel of the proteasome and the specificity of the process, many proteins and organelles cannot be degraded by the UPS. Autophagy is responsible for the bulk degradation of long-lived cytosolic proteins and organelles. Unlike proteasomal degradation, autophagic degradation is thought to be largely nonspecific. Portions of the cytoplasm are sequestered within cytosolic double-membrane vesicles, the autophagosomes, and damaged proteins and organelles are delivered to the lysosome (11). Autophagy is a major homeostatic and quality control mechanism to maintain cellular integrity (11). Thus, constitutive autophagy has been shown to function as a cell-repair mechanism that is particularly important for long-lived postmitotic cells such as neurons (11). Similar to neurons, podocytes are terminally differentiated cells, and autophagosomes have been shown to be present in podocytes in vitro (13), in mice (14), and in human renal biopsies (15). However, the functional significance of autophagy for glomerular development, maintenance, and disease progression has remained unknown.
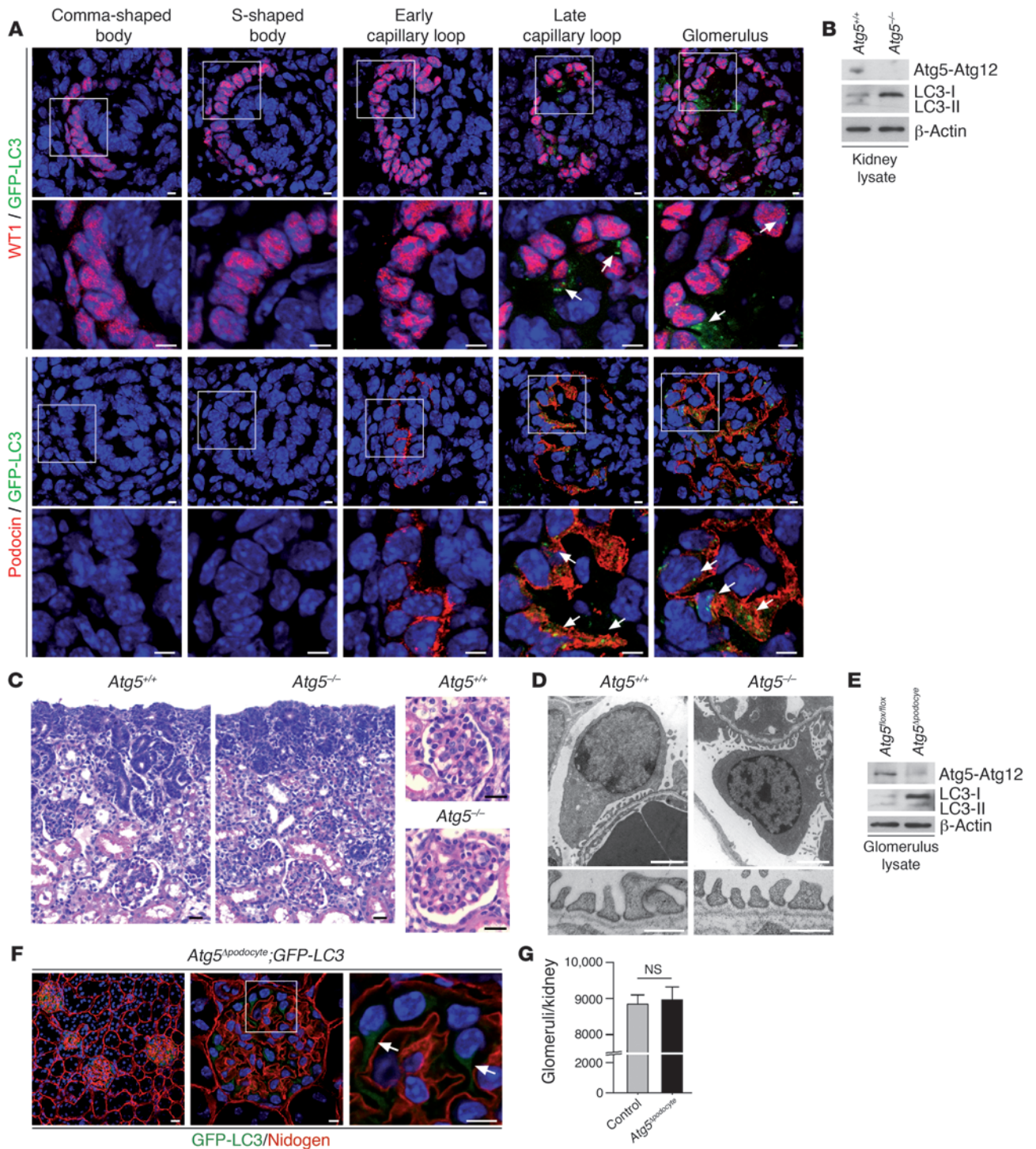
Here we demonstrate the critical role of autophagy for glomerular maintenance in aging glomeruli. Moreover, these data provide the first evidence that glomerular injury — a major risk factor for ESRD (5) — triggers autophagy to prevent the progression of glomerular disease. The dynamic regulation of protein degradative pathways in the podocyte appears to be a general theme for glomerular aging and glomerular disease progression.

## Results

*Glomerular podocytes exert high levels of autophagy under basal conditions.* We hypothesized that the postmitotic podocyte depends on autophagy to maintain cellular homeostasis, and we used transgenic mice expressing the fluorescent microtubule-associated protein 1 light chain 3, GFP-LC3, an autophagosome marker, to monitor autophagy in vivo (14). Strikingly, only glomerular podocytes displayed clearly detectable levels of autophagosomes within the kidney under basal conditions (Figure 1, A and B). Moreover, podocytes exerted unusually high levels of autophagosomes compared with other kidney cells (Figure 1C). However, increased numbers of autophagic vacuoles do not necessarily correlate with increased autophagic activity or flux, as such an increase can also result from impaired autophagosome/lysosome fusion or constitutively low lysosomal activity. To study the actual rate of autophagosome formation in podocytes, we generated a podocyte cell line expressing GFP-LC3. Blockade of autophagosomal degradation with the lysosomal inhibitor chloroquine induced a rapid accumulation of GFP-LC3–positive autophagosomes in GFP-LC3–expressing differentiated podocytes (Figure 1D). Autophagic flux rates of differentiated podocytes and inner medullary collecting duct (IMCD) cells were compared. Densitometric analysis of Western blots from cells incubated with chloroquine showed a significantly faster accumulation of converted LC3-II in podocytes, indicating a high rate of autophagic flux under non-starving conditions (Figure 1, E and F).

*Autophagy-related 5-dependent autophagy is dispensable for glomerular development.* To analyze the autophagic activity during podocyte differentiation, kidney sections of newborn transgenic *GFP-LC3* mice were stained with the podocyte nucleus marker WT1 and the foot process marker podocin. Since glomerular development

**Figure 2**
*Atg5*-dependent autophagy is dispensable for glomerular development. (**A**) Immunofluorescence staining of kidney sections derived from newborn *GFP-LC3*–transgenic mice identified autophagosomes during late podocyte differentiation in the late capillary loop stage. WT1 served as a marker for podocyte nuclei. Podocin served as a marker for podocyte foot processes. Arrows indicate GFP-LC3–positive autophagosomes. (**B**) Western blot analysis confirmed Atg5 deficiency in kidneys from *Atg5$^{-/-}$* mice by demonstrating the absence of Atg5 and the lack of LC3 conversion. (**C** and **D**) No morphological abnormalities of glomerular differentiation were detected in histology (**C**) or electron microscopy (**D**) of samples derived from fetal kidneys of *Atg5$^{-/-}$* mice. (**E**) Western blot analysis of isolated glomeruli from *Atg5$^{\Delta podocyte}$* mice confirmed the absence of Atg5 and displayed the abrogated conversion of LC3-I. (**F**) *Atg5$^{\Delta podocyte}$* mice were crossed with *GFP-LC3*–transgenic mice to confirm the functional ablation of autophagy. In these triple-transgenic mice, glomerular GFP-LC3–positive vesicles were completely absent and GFP-LC3 was diffusely distributed in the cytoplasm (arrows indicate cytosolic GFP signal). (**G**) No differences in the total number of glomeruli were detected in kidneys of *Atg5$^{\Delta podocyte}$* mice or control littermates (*P* = 0.78, 2-tailed Student's *t* test, *n* = 5 for each condition). Scale bars: 5 μm (**A** and **F**, middle and right), 20 μm (**C** and **F**, left), 2 μm (**D**, top), 500 nm (**D**, bottom).
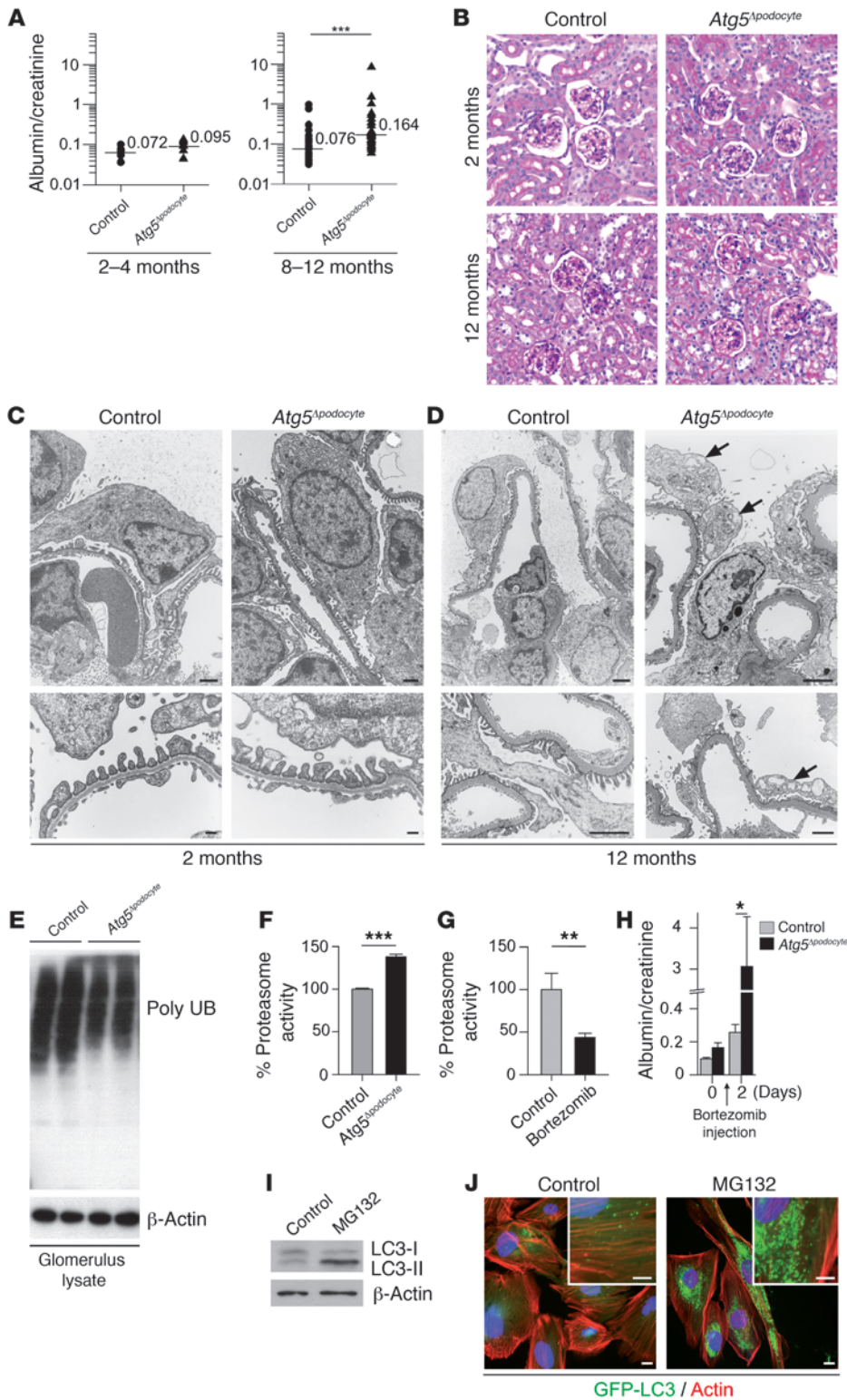
occurs asynchronously, all glomerular developmental stages were monitored on day 1 kidney sections. GFP-LC3–positive autophagosomes were not detected before late podocyte differentiation in the late capillary loop stage (Figure 2A). To further elucidate the role of autophagy in podocyte development, we analyzed constitutive autophagy-related 5 (Atg5) knockout mice (16). Glomeruli and podocytes in kidneys from Atg5-deficient E19 embryos (Atg5^{-/-}) showed no morphological abnormalities in histology and electron microscopy despite loss of LC3 conversion, indicating that the autophagic activity of podocytes is not required for their normal differentiation (Figure 2, B–D). We next generated podocyte-specific Atg5 knockout mice (Atg5[Δpodocyte]) by crossing Atg5-floxed mice (Atg5[flox/flox]) with podocin-Cre mice (17). In podocin-Cre–positive mice, floxed alleles are selectively excised in glomerular podocytes during late glomerular development (18). Western blot analysis from isolated glomeruli confirmed the almost complete loss of glomerular Atg5 and accumulation of LC3-I (Figure 2E), thus confirming that the high levels of autophagy observed in the glomerulus can be attributed to podocytes. To confirm the ablation of autophagy in podocytes, the Atg5[Δpodocyte] mice were subsequently crossed to GFP-LC3 transgenic mice. In these triple transgenic mice, glomerular GFP-LC3–positive vesicles were completely absent and GFP-LC3 was distributed diffusely in the cytoplasm (Figure 2F and Supplemental Figure 1; supplemental material available online with this article; doi:10.1172/JCI39492DS1). Like in the constitutive Atg5 knockout animals, the kidneys of newborn Atg5[Δpodocyte] mice displayed no obvious histological abnormalities (data not shown). Glomerulus counts of kidneys from Atg5[Δpodocyte] mice and control littermates were almost identical, indicating that podocyte-specific Atg5 deletion did not affect the number of developing nephrons (Figure 2G). However, these results do not exclude the possibility that Atg5-independent autophagy might compensate for correct development in Atg5-deficient animals (19).

*Functional cross-talk between the ubiquitin proteasome pathway and autophagy in podocytes.* To determine the physiological role of autophagy in podocytes, we analyzed Atg5[Δpodocyte] and control mice in age-matched groups. Up to 2–4 months after birth, Atg5[Δpodocyte] mice were indistinguishable from control littermates as analyzed by kidney histology, albuminuria, and glomerular ultrastructure (Figure 3, A–C). In an 8- to 12-month follow-up, Atg5[Δpodocyte] mice developed albuminuria that was mild but significantly higher than in control mice (Figure 3A). Interestingly, acute induction of podocyte-specific Atg5 knockout in 12-week-old doxycycline-inducible Atg5[flox/flox];Podocin-rtTA[+];tetO-Cre[+] mice caused a rapid onset of albuminuria, suggesting that the constitutive loss of Atg5 might be partially compensated by other pathways such as chaperone-mediated autophagy (20), Atg5-independent autophagy (19), or an upregulated proteasome activity (21) (Supplemental Figure 2). No obvious histological phenotype was detectable in 12-month-old podocyte-specific Atg5 knockout mice (Figure 3B). However, electron microscopy analysis identified significant changes, including vacuolar degeneration and large cystic structures (Figure 3D) in 12-month-old mice. Similar changes could already be seen in 8-month-old mice (data not shown). Further magnification revealed additional ultrastructural abnormalities such as cisternal distension of rough ER and aberrant membranous structures similar to those observed in Atg7-deficient livers (22), suggesting an abnormal turnover of organelles (Supplemental Figure 3). Surprisingly, and in contrast to many other tissues (17, 21–25), the genetic ablation of autophagy did not cause a

significant accumulation of poly-ubiquitinated proteins in the glomeruli of 8-month-old mice (Figure 3E). Although podocytes account for less than 20% of all glomerular cells, podocyte-specific deletion of autophagy resulted in a remarkable increase of total glomerular proteasome activity in these mice, as measured by chymotrypsin-like activity (Figure 3F), suggesting that the enhanced proteasome activity antagonizes an accumulation of poly-ubiquitinated proteins. To test the concept of a compensatory action of the proteasome in Atg5[Δpodocyte] animals in vivo, Atg5[Δpodocyte] and control mice were injected with the proteasome inhibitor bortezomib. Bortezomib injection resulted in a significant decrease of proteasome activity in total kidney lysates (Figure 3G) and caused a significant albuminuria in 6-month-old Atg5[Δpodocyte] mice compared with control littermates 24 hours after injection (Figure 3H). A functional coupling of autophagy and the UPS was also suggested by the fact that inhibition of the UPS by MG132 resulted in an increased autophagic activity, as documented by the conversion of cytoplasmic LC3-I into the membrane-bound LC3-II (Figure 3I) and the formation of GFP-LC3–positive autophagosomes in GFP-LC3–expressing differentiated podocytes (Figure 3J).

*Atg5 deficiency results in age-dependent late-onset glomerulosclerosis.* In a 20- to 24-month follow-up, Atg5[Δpodocyte] mice developed a progressive decline in glomerular function as evidenced by proteinuria (Figure 4A). Upon histology, 20- to 24-month-old Atg5[Δpodocyte] mice displayed significantly increased segmental or complete glomerular sclerosis compared with control littermates (Figure 4, B and C). In agreement with the measured proteinuria, proteinaceous casts and tubular dilatation were seen (Figure 4B). The expression and targeting of slit diaphragm proteins in non-sclerosed glomeruli displayed by immunofluorescence and specific immunogold stainings for nephrin and podocin seemed not to be severely affected, indicating that the glomerulopathy was not primarily caused by a defective slit diaphragm function (Supplemental Figure 4). Electron microscopy analysis revealed extensive vacuolar degeneration of podocyte cell bodies and foot process fusion (Figure 4D). Many of the vacuoles consisted of expanded ER lumens (Figure 4D). Furthermore, Atg5[Δpodocyte] podocytes displayed typical features of aging cells, such as signs of mitochondrial damage (Figure 4E), and accumulation of intra-lysosomal indigestible material, such as lipofuscin (Figure 4, F and G).

*ER stress and the accumulation of oxidized and ubiquitinated protein aggregates result in a loss of podocytes in Atg5[Δpodocyte] mice.* The dilated ER lumens stained positive for Calnexin by immunofluorescence (Figure 5A), indicating ER stress, which was confirmed by the detection of upregulated ER stress markers from isolated glomeruli of Atg5[Δpodocyte] mice (Figure 5B). Interestingly, the proteasomal activity of glomeruli from these Atg5[Δpodocyte] mice was significantly reduced compared with glomeruli from control mice (Figure 5C). In agreement with the reduced proteasomal activity, Western blot analysis (here shown as a short exposure) demonstrated a significant accumulation of poly-ubiquitinated proteins in glomeruli of Atg5[Δpodocyte] mice (Figure 5D). Accumulation of ubiquitin and the lysosomal marker Lamp2 was also confirmed by confocal microscopy (Supplemental Figure 5, A and B). In addition, a dramatic accumulation of p62/SQSTM1, a ubiquitin-binding scaffold protein that colocalizes with ubiquitinated protein aggregates in many neurodegenerative diseases (26), was detected, and p62 seemed to be deposited in larger aggregates as shown by immunofluorescence (Figure 5, E and F). These data suggest that the incremental accumulation of toxic proteins and altered organelles in autophagy-
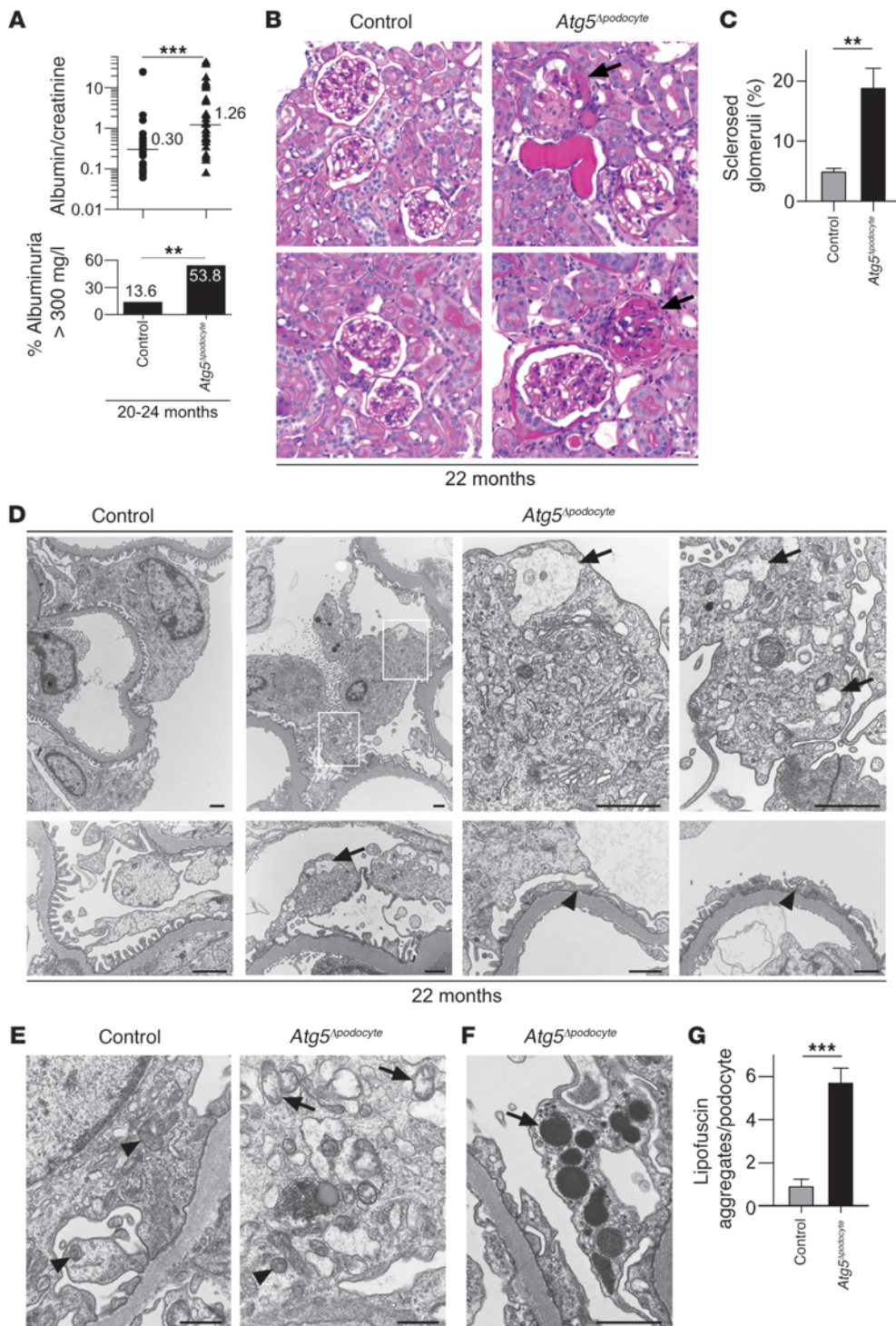
**Figure 3**
Functional cross-talk between the ubiquitin proteasome pathway and autophagy in podocytes. (**A**) Results from a 12-month follow-up of $Atg5^{\Delta podocyte}$ mice for proteinuria (2- to 4-month-old mice: $n = 6$ control mice, $n = 8$ $Atg5^{\Delta podocyte}$ mice; 8- to 12-month-old mice: $n = 34$ control mice, $n = 33$ $Atg5^{\Delta podocyte}$ mice; ***$P < 0.0001$ by 1-tailed Mann-Whitney $U$ test, $z = 4.16$). (**B**) No obvious histological phenotype in 2- to 4-month-old mice or in 8- to 12-month-old mice. (**C** and **D**) Electron microscopy analysis identified significant changes including vacuolar degeneration and ER extension (arrows indicate vacuoles) in 8- to 12-month-old $Atg5^{\Delta podocyte}$ mice. (**E**) There was no accumulation of ubiquitinated proteins in glomerulus lysate of 8-month-old $Atg5^{\Delta podocyte}$ mice. (**F**) Significant increase of proteasome activity in glomerulus lysate of 8-month-old $Atg5^{\Delta podocyte}$ mice (***$P < 0.001$, by ANOVA/Scheffe test; glomeruli from $n = 3$ control mice and $n = 3$ $Atg5^{\Delta podocyte}$ mice). (**G**) Significant decrease of proteasome activity in total kidney lysate of wild-type mice 24 hours after intravenous injection with the proteasome inhibitor bortezomib compared with control mice injected with 0.9% NaCl (**$P < 0.01$, by 2-tailed Student's $t$ test, kidney lysates from $n = 3$ control and $n = 6$ bortezomib mice). (**H**) Significant albuminuria of $Atg5^{\Delta podocyte}$ mice 24 hours after bortezomib injection (*$P < 0.05$, by 2-tailed Student's $t$ test; $n = 4$ control and $n = 3$ $Atg5^{\Delta podocyte}$ mice). (**I** and **J**) Inhibition of the proteasome with MG132 in differentiated podocytes resulted in an increase of converted LC3-II protein and an accumulation of GFP-LC3–positive autophagosomes. Scale bars: 20 μm (**B** and **J**), 1 μm (**C**, top), 200 nm (**C**, bottom), 2 μm (**D**); 10 μm (**J**, insets).

deficient podocytes might ultimately overwhelm the proteasome-dependent compensatory protein degradation, resulting in podocyte injury and glomerulosclerosis. Since the deposits of damaged proteins and altered organelles are particularly detrimental in non-dividing cells, autophagy-deficient podocytes share strik-

ing characteristics with aging neurons (17, 23, 27). Accumulation of oxidized proteins is widely considered a hallmark of aging in many tissues (28). To quantitatively assess the accelerated process of cellular aging, we measured the content of oxidized proteins in $Atg5^{\Delta podocyte}$ mice. Indeed, glomeruli from 22-month-old $Atg5^{\Delta podocyte}$
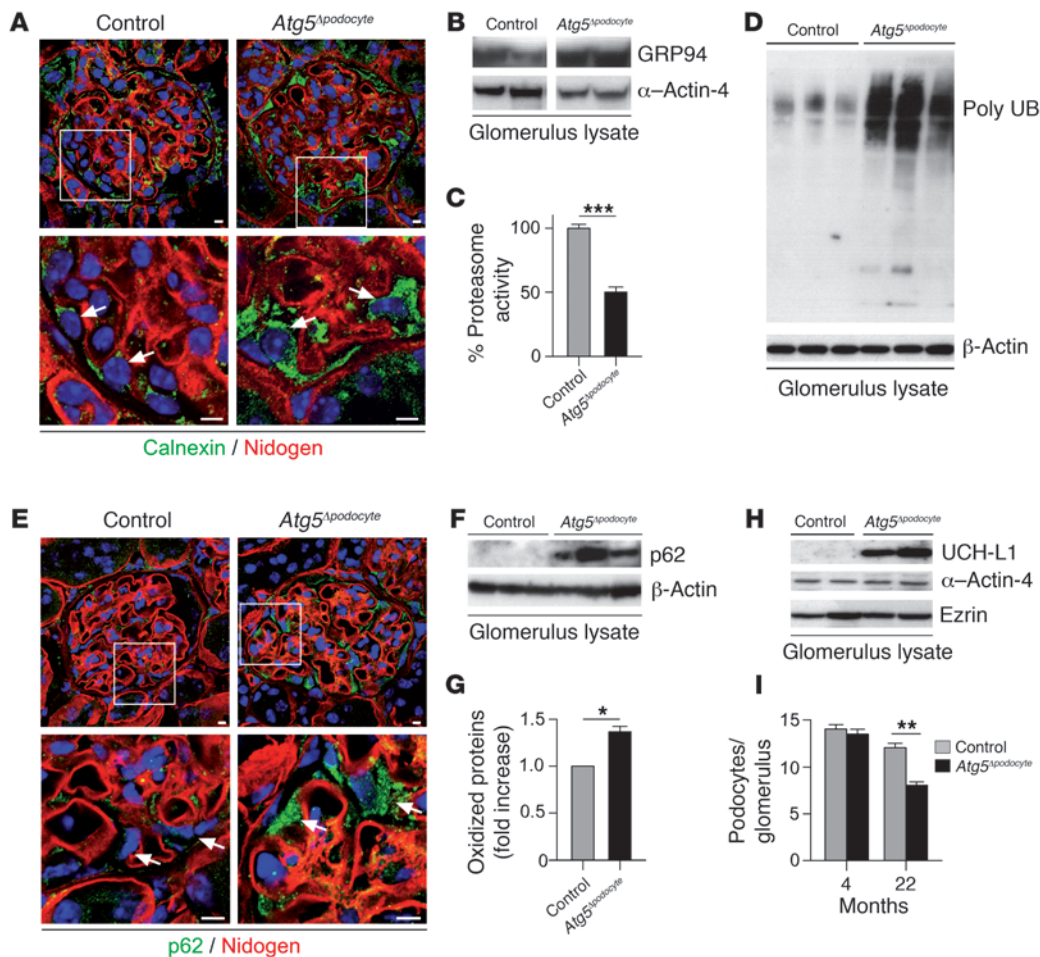
**Figure 4**
*Atg5* deficiency results in an age-dependent late-onset glomerulosclerosis. (**A**) Results from a 24-month follow-up of *Atg5^ΔPodocyte* mice for proteinuria (20- to 24-month-old mice; \*\*\*P < 0.001, by 1-tailed Mann-Whitney *U* test, z = 3.3, n = 22 control and n = 26 *Atg5^ΔPodocyte* mice; \*\*P = 0.004, by Fishers exact test). (**B**) On histology, 22-month-old *Atg5^ΔPodocyte* mice displayed segmental and complete glomerulosclerosis and proteinaceous casts with tubular dilatation (arrows indicate glomerulosclerosis). (**C**) Statistical analysis of sclerosed glomeruli (\*\*P = 0.0068, by 2-tailed Student's *t* test; glomeruli of n = 5 control and n = 7 *Atg5^ΔPodocyte* mice, 75 glomeruli of each mouse were analyzed). (**D–G**) Electron microscopy analysis revealed (**D**) extensive vacuolar degeneration of podocyte cell bodies and foot process fusion (arrows indicate vacuoles, arrowheads indicate foot process fusion), (**E**) damaged mitochondria (arrowheads indicate regular mitochondria, arrows indicate damaged mitochondria), and (**F** and **G**) lipofuscin accumulation (arrows indicate lipofuscin aggregates) (\*\*\*P < 0.0001, by 2-tailed Student's *t* test, podocytes of n = 3 control and n = 4 *Atg5^ΔPodocyte* mice). Scale bars: 20 μm (**B**), 1 μm (**D**), 500 nm (**E**), 1 μm (**F**).

mice significantly accumulated oxidized proteins compared with glomeruli from control animals (Figure 5G). In terminally differentiated neurons, several ubiquitin-associated proteins such as the ubiquitin carboxyterminal hydrolase L1 (UCH-L1) are known to be involved in the pathogenesis of neurodegenerative diseases and neuronal aging (11, 29). UCH-L1, recently identified in podocytes (30), was dramatically upregulated in glomeruli from autophagy-deficient mice (Figure 5H). To asses whether the podocyte damage

was accompanied by a loss of podocytes, we compared the number of glomerular podocytes from control and *Atg5^ΔPodocyte* mice at different ages. Indeed, a significantly reduced number of podocytes was already detected in non-sclerosed glomeruli of 22-month-old *Atg5^ΔPodocyte* mice, indicating that podocyte loss precedes the development of glomerulosclerosis (Figure 5I). These results clearly demonstrate the importance of basal, constitutive autophagy in maintaining glomerular function in aging mice.
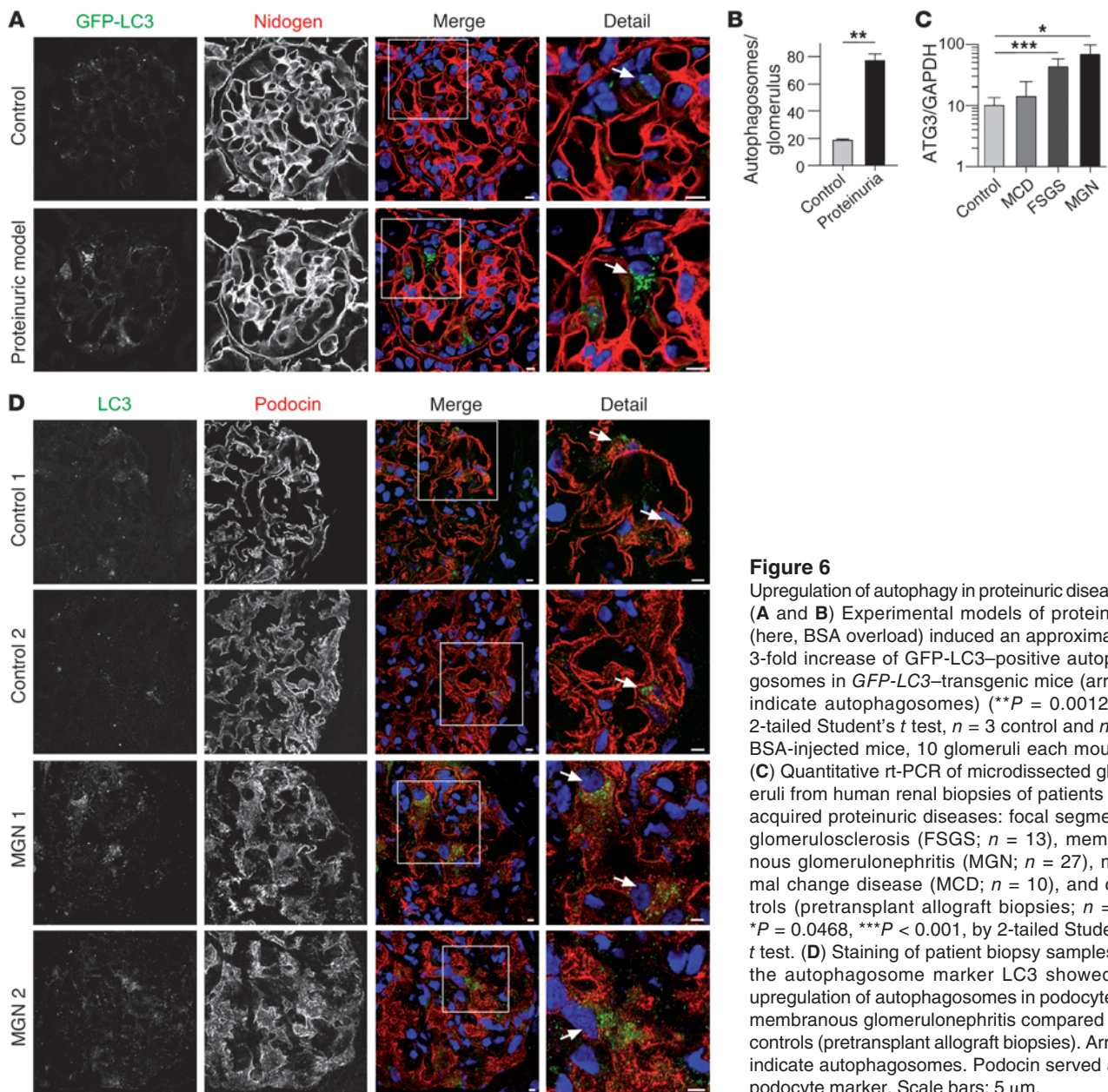
**Figure 5**

ER stress and the accumulation of oxidized and ubiquitinated protein aggregates result in a loss of podocytes in *Atg5Δpodocyte* mice. (**A**) Vacuolized podocytes stained positive for the ER marker calnexin (arrows indicate podocytes). (**B**) ER stress was confirmed by the increased detection of the ER stress marker GRP94 from lysates of isolated glomeruli. (**C**) The proteasomal activity of glomerular lysates of 22-month-old *Atg5Δpodocyte* mice was significantly reduced compared with control mice (***$P < 0.001$, by ANOVA/Scheffe test: glomeruli from $n = 3$ control and $n = 3$ *Atg5Δpodocyte* mice). (**D**) Short exposures of Western blots with glomerular lysates from 22-month-old control and *Atg5Δpodocyte* mice showed a significant accumulation of poly-ubiquitinated proteins. (**E** and **F**) Accumulation of the ubiquitin-associated protein p62 in *Atg5Δpodocyte* mice (arrows indicate podocytes). (**G** and **H**) Glomeruli from 22-month-old *Atg5Δpodocyte* mice accumulated oxidized proteins (*$P = 0.0186$, by 2-tailed Student's *t* test, glomeruli from $n = 3$ control and $n = 3$ *Atg5Δpodocyte* mice) and significantly upregulated the podocyte stress marker UCH-L1. (**I**) Loss of podocytes was reflected by reduced podocyte numbers per glomeruli in non-sclerosed glomeruli of 22-month-old *Atg5Δpodocyte* mice compared with control mice (**$P = 0.0026$, by 2-tailed Student's *t* test, glomeruli from $n = 3$ control and $n = 3$ *Atg5Δpodocyte* mice; 30 glomeruli for each mouse were analyzed). Scale bars: 5 μm (**A**), 5 μm (**E**).

*Upregulation of autophagy in proteinuric diseases.* The late onset of proteinuria in *Atg5Δpodocyte* mice enabled us to study the role of autophagy during glomerular injury. First we explored whether proteinuria leads to changes of autophagosome formation in *GFP-LC3; Atg5WT/WT* mice. Application of BSA overload induced an approximately 3-fold increase of GFP-LC3–positive autophagosomes (Figure 6, A and B), indicating a role for autophagy in response to proteinuria. To examine the role of autophagy in human kidney disease, we examined *ATG3* mRNA levels using quantitative real-time PCR (rt-PCR) in microdissected glomeruli from patients with acquired proteinuric diseases (31). Intriguingly, *ATG3* mRNA levels were 4- and 10-fold higher in podocytes from patients with focal segmental glomerulosclerosis and membranous glomerulonephritis compared with control samples (Figure 6C). Immunofluorescence

staining of 2 patient biopsy samples for the autophagosome marker LC3 showed an upregulation of autophagosomes in podocytes in membranous glomerulonephritis compared with controls (pretransplant allograft biopsies) (Figure 6D).

*Autophagy is critically involved in podocyte stress adaptation.* Autophagy can have opposing effects on cell survival (32). To clarify the role of induced autophagy in glomerular stress, we applied several glomerular disease models on non-proteinuric young (4–6 months old) *Atg5Δpodocyte* and control mice. Injection of puromycin aminonucleoside (PAN) (33, 34) or Adriamycin (35) resulted in a tremendous increase of albuminuria in young, non-proteinuric *Atg5Δpodocyte* mice compared with control littermates (Figure 7, A and E), with the subsequent development of glomerulosclerosis (Figure 7, B and F), foot process fusion (Figure 7, C and G), and loss of podocytes (Fig-

**Figure 6**
Upregulation of autophagy in proteinuric diseases. (**A** and **B**) Experimental models of proteinuria (here, BSA overload) induced an approximately 3-fold increase of GFP-LC3–positive autophagosomes in *GFP-LC3*–transgenic mice (arrows indicate autophagosomes) (**$P = 0.0012$, by 2-tailed Student's $t$ test, $n = 3$ control and $n = 4$ BSA-injected mice, 10 glomeruli each mouse). (**C**) Quantitative rt-PCR of microdissected glomeruli from human renal biopsies of patients with acquired proteinuric diseases: focal segmental glomerulosclerosis (FSGS; $n = 13$), membranous glomerulonephritis (MGN; $n = 27$), minimal change disease (MCD; $n = 10$), and controls (pretransplant allograft biopsies; $n = 9$). *$P = 0.0468$, ***$P < 0.001$, by 2-tailed Student's $t$ test. (**D**) Staining of patient biopsy samples for the autophagosome marker LC3 showed an upregulation of autophagosomes in podocytes in membranous glomerulonephritis compared with controls (pretransplant allograft biopsies). Arrows indicate autophagosomes. Podocin served as a podocyte marker. Scale bars: 5 μm.

ure 7, D and H), indicating that loss of autophagy dramatically sensitized animals toward the development of glomerular diseases. In addition, low doses of BSA (36, 37) or LPS (38) caused significantly higher transient albuminuria in *Atg5$^{\Delta podocyte}$* mice compared with control littermates (Supplemental Figure 6).
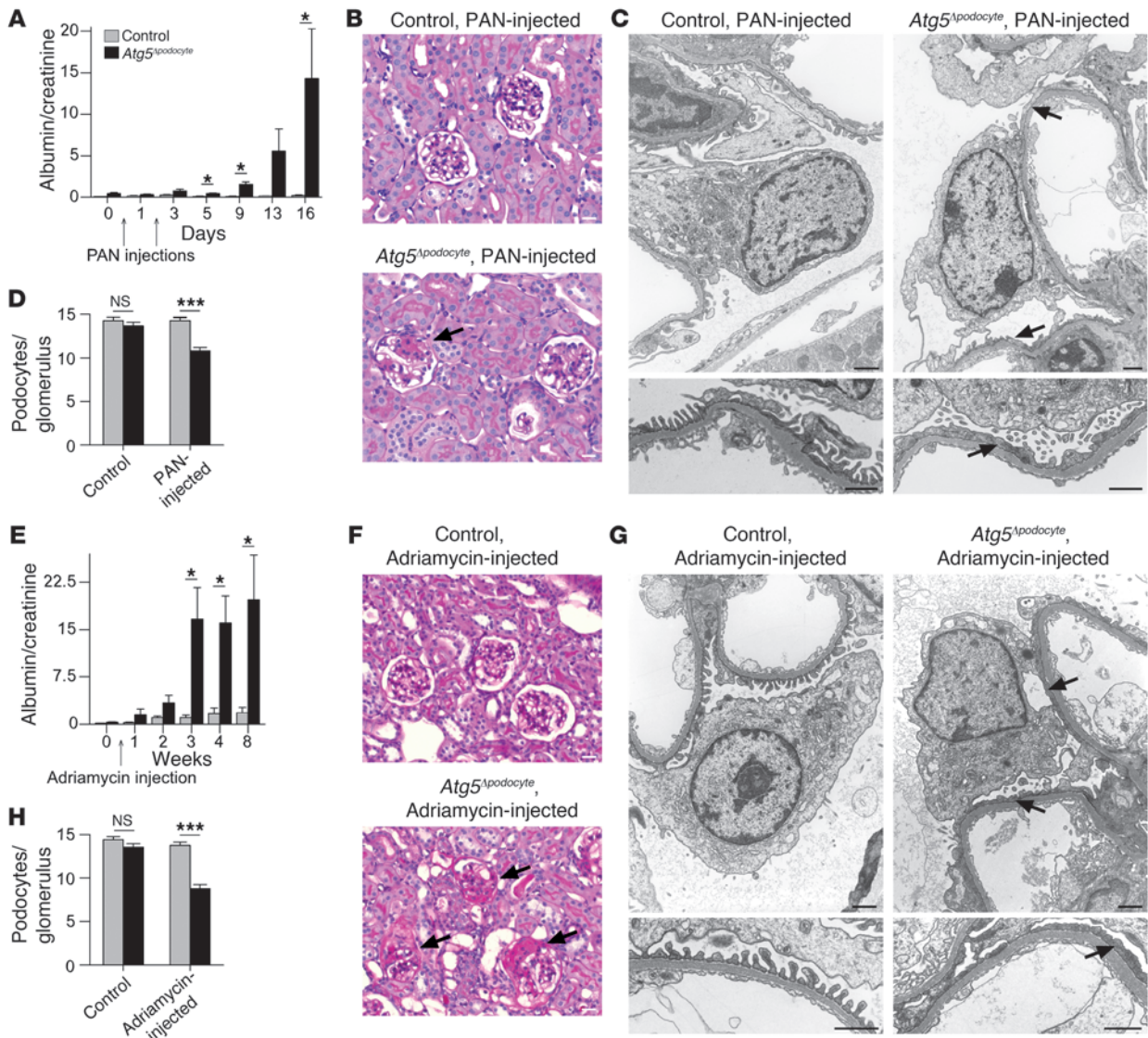
These findings strongly support the hypothesis that autophagy defends the integrity of podocytes against glomerular disease progression (illustrated in Supplemental Figure 7).

## Discussion

Autophagy is a cellular pathway involved in protein and organelle degradation with an amazing number of connections between cellular homeostasis and human disease (11). Our results here highlight the critical role of autophagy as a determinant of glomerular aging and glomerular disease (illustrated in Supplemental Figure 7).

Glomerular diseases are primarily responsible for the rising costs associated with ESRD worldwide (5). Due to its complexity and its postmitotic nature, the podocyte represents the most fragile component of the glomerular filtration barrier. In most human glomerulopathies, podocyte foot process effacement is a hallmark of glomerular injury leading to proteinuria (39). Failures of reparative mechanisms promote persistent proteinuria and the development of glomerulosclerosis (39). Unfortunately, very little has been known on the molecular nature of the reparative mechanisms that defend the podocyte against environmental stress and cellular aging. The understanding of this missing link could be the basis for successful therapeutic prevention of irreversible glomerulosclerosis. Our data now reveal autophagy as an important mechanism for podocyte homeostasis. Autophagy has previously been shown to be an essential cell repair and turnover mecha-

**Figure 7**
Autophagy is critically involved in podocyte stress adaptation. (**A**) Injection of PAN resulted in a dramatic increase of albuminuria in non-proteinuric 6-month-old $Atg5^{\Delta podocyte}$ mice compared with control mice ($n$ = 6 for control and for $Atg5^{\Delta podocyte}$ mice, *$P$ < 0.05, by 2-tailed Student's $t$ test). (**B–D**) PAN injection in $Atg5^{\Delta podocyte}$ mice resulted in (**B**) glomerulosclerosis in PAS staining (arrow indicates a sclerosed glomerulus), (**C**) foot process fusion in electron microscopy (arrows indicate fused foot processes), and (**D**) loss of podocytes (***$P$ < 0.001, by 2-tailed Student's $t$ test, glomeruli from $n$ = 4 control and $n$ = 4 $Atg5^{\Delta podocyte}$ mice; 30 glomeruli for each mouse were analyzed). (**E–H**) Injection of Adriamycin resulted in (**E**) a significant increase of albuminuria in non-proteinuric 6-month-old $Atg5^{\Delta podocyte}$ mice compared with control littermates ($n$ = 6 for control and for $Atg5^{\Delta podocyte}$ mice, *$P$ < 0.05, by 2-tailed Student's $t$ test), and in (**F**) glomerulosclerosis (PAS staining, arrows mark segmental sclerosed glomeruli), (**G**) foot process fusion in electron microscopy (arrows indicate fused foot processes), and (**H**) loss of podocytes (***$P$ < 0.001, by 2-tailed Student's $t$ test, glomeruli from $n$ = 3 control and $n$ = 3 $Atg5^{\Delta podocyte}$ mice; 30 glomeruli for each mouse were analyzed). Scale bars: 20 μm (**B** and **F**), 1 μm (**C** and **G**).

nism for postmitotic cells such as neurons (10, 11). Strikingly, in the kidney, glomerular podocytes most prominently display autophagic activity. Atg5-deficient podocytes that are incapable of performing autophagy progressively accumulate biological "garbage" such as damaged mitochondria and ubiquitinated protein aggregates, underlining that the removal of this cellular waste depends on autophagy in podocytes. The compromised clearance of old and/or damaged mitochondria by autophagy coupled with reduced turnover of long-lived proteins probably contributes to

the intracellular accumulation of oxidized proteins seen in Atg5-deficient podocytes. Podocytes are particularly susceptible to oxidative injury (40). Both ER stress and oxidative stress ultimately lead to irreversible podocyte injury and podocyte loss. This clearly distinguishes podocytes from other glomerular structures that are efficiently renewed due to proliferation, providing a dilution of oxidatively or otherwise damaged proteins and cell organelles.

The efficiency of autophagy seems to be a direct determinant of cellular aging for long-lived glomerular podocytes. Indeed,

autophagy-deficient podocytes perfectly phenocopied many age-related cellular alterations (Figures 4 and 5). Most prominent signs of this accelerated aging in Atg5-deficient podocytes are the accumulation of lipofuscin, the formation of ubiquitinated protein aggregates and aggresomes, the occurrence of damaged mitochondria, and the increase in the load of oxidized proteins. To our knowledge this is the first genetic mouse model clearly featuring an aging podocyte. Aging in humans and rodents progressively impairs renal function (5, 8, 41). The age-related structural kidney changes are characterized by loss of podocytes and glomerulosclerosis (5, 42). The exact mechanisms underlying age-dependent renal injury are unknown. Even in the absence of known risk factors such as hypertension or diabetes, otherwise healthy individuals (65 years old or older) frequently present glomerulosclerosis (5). The autophagy-lysosome system undergoes striking changes in aging cells. Aging in general leads to a reduction in autophagosome formation and autophagosome-lysosome fusion (10, 43). It is intriguing to speculate that a gradual decrease of glomerular autophagic activity with age could play a major role in the functional decline of renal function in human aging kidneys.

In most cases, the ultimate fate of defective proteins identified by quality control systems is degradation by either the autophagy-lysosome system or the UPS. Both of these degradation pathways have been implicated in the pathogenesis of neurodegenerative disease (11). However, the UPS and autophagy were long viewed as independent degradation systems. Interestingly, in the podocyte the UPS and the autophagy-lysosome system appeared to be functionally coupled, as Atg5-deficient podocytes did exert highly upregulated proteasome activities at young ages and the occurrence of a more severe podocyte phenotype in old mice seemed to be correlated with the decline in compensatory proteasome activity. In addition, inhibition of the UPS resulted in an increased autophagic activity in wild-type podocytes. Similar induction of autophagy has been observed in response to genetic impairment of the proteasome in *Drosophila melanogaster* (44). These results might suggest that podocytes can switch between autophagy and the UPS, and that each system can at least partially maintain the clearance of intracellular degradation products in podocytes. One simple possible mechanism of such an autophagy-UPS interaction could be that the autophagic machinery directly degrades proteasomal components, which would explain the increased proteasomal activity in Atg5-deficient podocytes. Although unproven at this point, it seems possible that the upregulation of alternative proteolytic pathways in constitutively autophagy-deleted tissues contributes to the observed phenotypes not only in podocytes, but also in other tissues such as cardiomyocytes, where heart-specific constitutive and temporally controlled Atg5 deletion caused significantly different phenotypes (21). Thus, in contrast to the traditional notion of the UPS and autophagy providing discrete routes of degradation for short-lived and long-lived proteins, our data support recent findings indicating that a subset of proteins may be degraded by either pathway (45, 46).

Recently, it has been shown that autophagy can occur through an Atg5/Atg7-independent alternative pathway (19). This underlines the complexity of protein degradative pathways. Atg5-dependent macroautophagy has been demonstrated to be crucial for basal and starvation-induced autophagy (11), for neuronal protein aggregate clearance, and for stress adaptation (11, 21). In contrast,

the alternative Atg5-independent autophagy can be triggered by cellular stress in vitro and functions in the autophagic elimination of organelles during erythrocyte differentiation in vivo (19). In the future it will be important to further dissect the interplay of Atg5-dependent autophagy, Atg5-independent autophagy, chaperone-mediated autophagy, and other proteolytic pathways.

Despite the important function of basal autophagy in podocytes, the requirement for autophagy is even more evident under glomerular disease conditions. Our data show that the autophagic machinery is induced in proteinuric animal models as well as in human glomerular diseases. Since autophagy can have opposing effects on cell survival (32), we proofed whether this process is a causative or a compensatory mechanism by comparing models of glomerular stress in wild-type and *Atg5*^Δpodocyte^ mice. Intriguingly, autophagy deficiency dramatically sensitized podocytes toward glomerular stress. Thus, autophagy is a novel cellular stress surveillance factor for podocytes that appears to function both as a sensor of stress stimuli and as an effector, which coordinates podocyte homeostasis.

In summary, this study identifies basal autophagy as crucial factor for glomerular maintenance and glomerular aging (Supplemental Figure 7). In addition, we demonstrate the importance of induced autophagy in glomerular injury — a major risk factor for glomerular disease and end-stage kidney disease (5). It is very reasonable to assume that autophagy could be a novel therapeutic target (47) for the treatment of glomerular diseases. However, in any attempt at manipulating podocyte autophagy therapeutically, it will be important to acknowledge the dynamic nature of the changes that occur in the autophagic system and related protein degradative pathways during the course of glomerular disease.

## Methods

*Mice.* Mice bearing an *Atg5*^flox^ allele, in which exon 3 of the *Atg5* gene is flanked by 2 *loxP* sequences, have been previously reported (17). Podocin-*Cre* mice were provided by L. Holzman (Renal, Electrolyte and Hypertension Division, University of Pennsylvania School of Medicine, Philadelphia, PA, USA) (18). Atg5-floxed mice (*Atg5*^flox/flox^) were crossed with Podocin-*Cre* mice to generate podocyte-specific *Atg5* knockout mice *Atg5*^flox/flox^;Podocin-*Cre*^+^ (*Atg5*^Δpodocyte^). *Atg5*^flox/WT^;Podocin-*Cre*^+^ and *Atg5*^flox/flox^;Podocin-*Cre*^−^ littermates served as controls. *Atg5*^Δpodocyte^ mice were subsequently crossed to *GFP-LC3* transgenic mice. *Atg5* constitutive knockout mice (*Atg5*^−/−^) (16) and *GFP-LC3* transgenic mice (14) have been previously reported. All mice were crossed on a pure C57BL/6 background. The C57BL/6 strain, which is widely used as background for transgenic and knockout mouse models, is known to be relatively resistant to kidney injury (48), which might contribute to the late onset of glomerulosclerosis in C57BL/6 *Atg5*^Δpodocyte^ mice. Podocin-*rtTA*;tetO-*Cre* mice were provided by S. Quaggin (Samuel Lunenfeld Research Institute, Mount Sinai Hospital, University of Toronto, Canada) (49). To generate doxycycline-inducible podocyte-specific *Atg5* knockout mice (*Atg5*^flox/flox^;Podocin-*rtTA*^+^;tetO-*Cre*^+^) Atg5-floxed mice (*Atg5*^flox/flox^) were crossed with Podocin-*rtTA*;tetO-*Cre* mice. TetO-*Cre*^−^ littermates served as a control. For the induction of *Atg5* deletion, 12-week-old *Atg5*^flox/flox^;Podocin-*rtTA*^+^;tetO-*Cre*^+^ mice received doxycycline hydrochloride (Sigma-Aldrich) via drinking water (2 mg/ml with 5% sucrose, protected from light) for a total of 14 days. All animal studies were approved by the Committee on Research Animal Care, Regierungspräsidium Freiburg.

*Protein overload and subsequent analysis.* *Atg5*^Δpodocyte^ mice (*n* = 5) and control littermates (*n* = 6) received endotoxin-free BSA (Sigma-Aldrich; catalog A9430) (250 mg/ml, dissolved in PBS) intraperitoneally for 5 consecutive days with increasing dose (2, 4, 6, 8 and 10 mg/g body weight) (36, 37). Uri-

nary albumin excretion rates were analyzed before injections and at days 1 to 7 after the first injection. To monitor the induction of autophagy, *GFP-LC3* transgenic mice received either endotoxin-free BSA (*n* = 4) or the equivalent volume of PBS as control (*n* = 3) intraperitoneally for 7 consecutive days with increasing doses (2, 4, 6, 8, 10, 10, 10 mg/g body weight). Proteinuria was confirmed by urine dip-stix (≥20 g/l) and Coomassie gel. GFP-LC3–positive autophagosomes were quantified using ImageJ software.

*LPS-induced proteinuria.* Atg5<sup>Δpodocyte</sup> mice and control littermates (*n* = 4 each) were injected intraperitoneally with a single dose of 200 μg LPS (Sigma-Aldrich) (1 mg/ml in sterile PBS) in a total volume of 200 μl. Urinary albumin excretion rates were analyzed before the single dose injection and at days 1 and 3 after the injection and normalized to urinary creatinine (38).

*PAN-induced proteinuria.* Atg5<sup>Δpodocyte</sup> mice and control littermates (*n* = 6 each) received 2 doses of intravenous PAN (Sigma-Aldrich) in 0.9% NaCl (15 mg/ml) at day 0 and 2 (18.25 mg/100 g body weight) (33, 34). Urinary albumin excretion rates were analyzed before the 2 dose injections and at days 1, 3, 5, 9, 13, and 16 after the first injection. Kidneys were harvested and processed for PAS staining and electron microscopy after the 16-day follow-up.

*Adriamycin-induced proteinuria.* Atg5<sup>Δpodocyte</sup> mice and control littermates (*n* = 6 each) received 1 dose of intravenous Adriamycin (Sigma-Aldrich) in 0.9% NaCl (2 mg/ml) (15 μg/g body weight) (35). Urinary albumin excretion rates were analyzed before injection and 1, 2, 3, 4, and 8 weeks after injection. Kidneys were harvested and processed for PAS staining and electron microscopy after the 8-week follow-up.

*Bortezomib-induced proteinuria.* Atg5<sup>Δpodocyte</sup> mice (*n* = 3) and control littermates (*n* = 4) received 1 dose of intravenous bortezomib (Janssen-Cilag) in 0.9% NaCl (1 mg/ml) (1.5 μg/g body weight) (50). Urinary albumin excretion rates were analyzed before injection and 24 hours after injection.

*Urine analysis.* Urinary albumin and creatinine were measured using mouse albumin-specific ELISA (Bethyl) and creatinine kits. Proteinuria was expressed as mg albumin/mg creatinine. In addition, Coomassie gels were used to semi-quantitatively confirm the proteinuria (data not shown).

*Histological analysis.* Kidneys were fixed in 4% paraformaldehyde and embedded in paraffin or in Lowicryl K4M resin (Electron Microscopy Sciences) and further processed for PAS staining or electron microscopy, respectively. Kidneys of 12-day-old Atg5<sup>Δpodocyte</sup> mice and control littermates were fixed with 4% paraformaldehyde. Fixed kidneys were embedded in paraffin and totally sectioned into a complete set of consecutive slices of 8 nm on a Leica microtome. The total numbers of glomeruli per kidney were counted as previously described (51).

*Immunoelectron microscopy.* Kidneys of 22-month-old Atg5<sup>Δpodocyte</sup> mice and control littermates were fixed with 4% paraformaldehyde. Fixed samples were embedded in Lowicryl K4M resin (Electron Microscopy Sciences), and ultrathin sections were labeled by an indirect immunogold protocol, as described previously (52).

*Immunofluorescence staining of kidney sections.* Kidneys were frozen in OCT compound and sectioned at 6 μm (Leica Kryostat). The sections were fixed with 4% paraformaldehyde, blocked in PBS containing 5% BSA, and incubated for 1 hour with primary antibodies. After several PBS rinses, fluorophore-conjugated secondary antibodies (Invitrogen) were applied for 30 minutes. Confocal images were taken using a Zeiss laser scan microscope equipped with a ×63 water immersion objective. To determine the number of podocytes per glomeruli, kidney sections were stained against the podocyte nuclear marker WT1. WT1-positive cells were counted in 30 glomeruli per mouse per condition (*n* = 3 for each condition).

*Isolation and characterization of adult mouse glomeruli.* Glomeruli were isolated using Dynabead perfusion and were glass-glass homogenized in lysis buffer (containing 20 mM CHAPS and 1% Triton X-100) (53, 54). After centrifugation (15,000 *g* for 15 minutes at 4°C) protein concentration was determined by Dc Protein-Assay (Bio-Rad). Equal amounts of protein were separated by SDS-PAGE.

*Proteasome activity analysis.* Glomeruli were lysed in T-Per (Pierce Biotechnology Inc.) with Protease Complete Inhibitor cocktail without EDTA (Roche) (*n* = 3 for control and Atg5<sup>Δpodocyte</sup> mice). Protein concentration was determined by a standard bicinchoninic acid assay (Pierce Biotechnology Inc.) according to the manufacturer's instructions. For the measurement of proteasomal (chymotrypsin-like) activity, 10 μg total protein were diluted in incubation buffer (20 mM HEPES, 0.5 mM EDTA, 5 mM DTT, 0.1 mg/ml ovalbumin in $H_2O$, pH 7.8) to a final volume of 50 μl. Probes were preincubated in incubation buffer for 2 hours at 4°C. Following preincubation, the substrate Suc-LLVY-AMC (Calbiochem) was added to the probes at a final concentration of 60 μM and to an end volume of 100 μl. Proteasomal activity was measured in triplicate at 355 and 460 nm in a Mithras LB 940 fluorescent spectrophotometer after incubation at 37°C for 1 hour in the dark.

*Oxidized protein analysis.* The amount of oxidized proteins in homogenates of glomeruli was determined by using an OxyElisa Oxidized Protein Quantitation Kit (Chemicon) according to the manufacturer's instructions.

*Patients and quantitative glomerular rt-PCR.* Human renal biopsy specimens were procured in an international multicenter study, the European Renal cDNA Bank–Kroener-Fresenius Biopsy Bank (ERCB-KFB; members are listed in ref. 55). Biopsies were obtained from patients after informed consent and with approval of the local ethics committees. Microdissection, RNA isolation, reverse transcription, and rt-PCR were performed as described previously (31). Pre-developed TaqMan reagents were used for human ATG3 (NM_022488.3) and for reference genes (Applied Biosystems). In addition, 2 biopsy samples from histologically classified membranous nephropathy and 2 controls (pretransplant living donor biopsy) were used for immunofluorescence analysis.

*Cell culture.* Human and mouse podocyte cell lines were provided by M. Saleem (Children's Renal Unit, Bristol Royal Hospital for Children, University of Bristol, UK) and P. Mundel (Department of Medicine, University of Miami, Miller School of Medicine, Miami, FL, USA) and were cultured as previously described (56, 57). *GFP-LC3*–transgenic podocytes were generated by retroviral transduction of pMX-GFP-rat LC3 (58) as previously described (59, 60). For lysosomal inhibition, human podocytes and IMCD cells were incubated with chloroquine dissolved in PBS (25 μM final concentration) for 2, 4, and 6 hours. Western blots of cell lysates were stained against LC3 and CD2AP as loading control. Densitometric analysis of Western blots was performed with ImageJ software. For inhibition of the UPS, cells were incubated for 6 hours with MG132 dissolved in DMSO (25 μM final concentration) or DMSO as control.

*Antibodies.* Antibodies were obtained from Acris (anti-Nephrin guinea pig pAb, BP5030), Sigma-Aldrich (anti-podocin rabbit pAb, P0372; anti–β-actin mouse mAb, A5441; anti-ezrin mouse mAb, E8897), Chemicon (anti-nidogen rat mAb, MAB1946; anti-ubiquitin rabbit pAb, AB1690; anti-ubiquitin mouse mAb, MAB1510; anti–UCH-L1 rabbit pAb, AB1761), Abcam (anti-WT1 rabbit pAb, ab15249; anti-Lamp2 rabbit mAb, ab37024), Biomol (anti-calnexin rabbit pAb, SPA-860), Cell Signaling Biotechnology (anti-LC3B rabbit pAb, 2775; anti-human Atg12 rabbit pAb, 2010; anti-mouse Atg12 rabbit pAb, 2011), ImmunoGlobe (anti–α-actinin-4 rabbit pAb, 0042-05), Stressgen (anti-GRP94 rat mAb, SPA-850), MBL (anti-LC3 mouse mAb, M152-3), Cosmo Bio (anti-Atg5 rabbit pAb, TMD-PH-AT5) and Progen (anti-p62 guinea pig pAb, GP62-C). Anti-CD2AP rabbit pAb was described previously (61).

Secondary antibodies, actin, and nuclear staining reagents were obtained from Invitrogen (To-Pro-3, T3605; Alexa Fluor 546 phalloidin, A22283; Alexa Fluor 488 goat anti–guinea pig IgG, A11073; Alexa Fluor 555 goat anti-rat IgG, A21434; Alexa Fluor 488 goat anti-rat IgG; Alexa Fluor 488 donkey anti-rabbit, A21206).

*Statistics.* Data were expressed as the mean ± SEM. All experiments were performed at least 3 times. Statistical comparisons were performed with the program Statistica using ANOVA with the Scheffe test, 2-tailed Student's *t* test, 1-tailed Fisher's exact test, or 1-tailed Mann-Whitney *U* test. Differences with $P < 0.05$ were considered significant.

## Acknowledgments

Address correspondence to: Tobias B. Huber, Renal Division, University Hospital Freiburg, Breisacher Str. 66, 79106 Freiburg, Germany. Phone: 49.761.270.3559; Fax: 49.761.270.3270; E-mail: tobias.huber@uniklinik-freiburg.de.

1. Huber TB, Benzing T. The slit diaphragm: a signaling platform to regulate podocyte function. *Curr Opin Nephrol Hypertens*. 2005;14(3):211–216.
2. Pavenstadt H, Kriz W, Kretzler M. Cell biology of the glomerular podocyte. *Physiol Rev*. 2003; 83(1):253–307.
3. White KE, et al. Podocyte number in normotensive type 1 diabetic patients with albuminuria. *Diabetes*. 2002;51(10):3083–3089.
4. Lemley KV, et al. Podocytopenia and disease severity in IgA nephropathy. *Kidney Int*. 2002;61(4):1475–1485.
5. Wiggins RC. The spectrum of podocytopathies: a unifying view of glomerular diseases. *Kidney Int*. 2007;71(12):1205–1214.
6. Vogelmann SU, Nelson WJ, Myers BD, Lemley KV. Urinary excretion of viable podocytes in health and renal disease. *Am J Physiol Renal Physiol*. 2003; 285(1):F40–F48.
7. Skoberne A, Konieczny A, Schiffer M. Glomerular epithelial cells in the urine: what has to be done to make them worthwhile? *Am J Physiol Renal Physiol*. 2009;296(2):F230–F241.
8. Floege J, et al. Age-related glomerulosclerosis and interstitial fibrosis in Milan normotensive rats: a podocyte disease. *Kidney Int*. 1997;51(1):230–243.
9. Brandis A, Bianchi G, Reale E, Helmchen U, Kuhn K. Age-dependent glomerulosclerosis and proteinuria occurring in rats of the Milan normotensive strain and not in rats of the Milan hypertensive strain. *Lab Invest*. 1986;55(2):234–243.
10. Cuervo AM, Bergamini E, Brunk UT, Droge W, Ffrench M, Terman A. Autophagy and aging: the importance of maintaining "clean" cells. *Autophagy*. 2005;1(3):131–140.
11. Mizushima N, Levine B, Cuervo AM, Klionsky DJ. Autophagy fights disease through cellular self-digestion. *Nature*. 2008;451(7182):1069–1075.
12. Winslow AR, Rubinsztein DC. Autophagy in neurodegeneration and development. *Biochim Biophys Acta*. 2008;1782(12):723–729.
13. Asanuma K, et al. MAP-LC3, a promising autophagosomal marker, is processed during the differentiation and recovery of podocytes from PAN nephrosis. *FASEB J*. 2003;17(9):1165–1167.
14. Mizushima N, Yamamoto A, Matsui M, Yoshimori T, Ohsumi Y. In vivo analysis of autophagy in response to nutrient starvation using transgenic mice expressing a fluorescent autophagosome marker. *Mol Biol Cell*. 2004;15(3):1101–1111.
15. Sato S, Kitamura H, Adachi A, Sasaki Y, Ghazizadeh M. Two types of autophagy in the podocytes in renal biopsy specimens: ultrastructural study. *J Submicrosc Cytol Pathol*. 2006;38(2–3):167–174.
16. Kuma A, et al. The role of autophagy during the early neonatal starvation period. *Nature*. 2004; 432(7020):1032–1036.
17. Hara T, et al. Suppression of basal autophagy in neural cells causes neurodegenerative disease in mice. *Nature*. 2006;441(7095):885–889.
18. Moeller MJ, Sanden SK, Soofi A, Wiggins RC, Holzman LB. Podocyte-specific expression of cre recombinase in transgenic mice. *Genesis*. 2003;35(1):39–42.
19. Nishida Y, et al. Discovery of Atg5/Atg7-independent alternative macroautophagy. *Nature*. 2009; 461(7264):654–658.
20. Massey AC, Zhang C, Cuervo AM. Chaperone-mediated autophagy in aging and disease. *Curr Top Dev Biol*. 2006;73:205–235.
21. Nakai A, et al. The role of autophagy in cardiomyocytes in the basal state and in response to hemodynamic stress. *Nat Med*. 2007;13(5):619–624.
22. Komatsu M, et al. Impairment of starvation-induced and constitutive autophagy in Atg7-deficient mice. *J Cell Biol*. 2005;169(3):425–434.
23. Komatsu M, et al. Loss of autophagy in the central nervous system causes neurodegeneration in mice. *Nature*. 2006;441(7095):880–884.
24. Jung HS, et al. Loss of autophagy diminishes pancreatic beta cell mass and function with resultant hyperglycemia. *Cell Metab*. 2008;8(4):318–324.
25. Ebato C, et al. Autophagy is important in islet homeostasis and compensatory increase of beta cell mass in response to high-fat diet. *Cell Metab*. 2008; 8(4):325–332.
26. Bjorkoy G, et al. p62/SQSTM1 forms protein aggregates degraded by autophagy and has a protective effect on huntingtin-induced cell death. *J Cell Biol*. 2005;171(4):603–614.
27. Levine B, Kroemer G. Autophagy in the pathogenesis of disease. *Cell*. 2008;132(1):27–42.
28. Stadtman ER. Protein oxidation and aging. *Science*. 1992;257(5074):1220–1224.
29. Leroy E, et al. The ubiquitin pathway in Parkinson's disease. *Nature*. 1998;395(6701):451–452.
30. Meyer-Schwesinger C, et al. A new role for the neuronal ubiquitin C-terminal hydrolase-L1 (UCH-L1) in podocyte process formation and podocyte injury in human glomerulopathies. *J Pathol*. 2009; 217(3):452–464.
31. Cohen CD, Frach K, Schlondorff D, Kretzler M. Quantitative gene expression analysis in renal biopsies: a novel protocol for a high-throughput multicenter application. *Kidney Int*. 2002;61(1):133–140.
32. Shintani T, Klionsky DJ. Autophagy in health and disease: a double-edged sword. *Science*. 2004;306(5698):990–995.
33. Kerjaschki D, Vernillo AT, Farquhar MG. Reduced sialylation of podocalyxin--the major sialoprotein of the rat kidney glomerulus--in aminonucleoside nephrosis. *Am J Pathol*. 1985;118(3):343–349.
34. Nakajo A, et al. Mizoribine corrects defective nephrin biogenesis by restoring intracellular energy balance. *J Am Soc Nephrol*. 2007;18(9):2554–2564.
35. Wang Y, Wang YP, Tay YC, Harris DC. Progressive adriamycin nephropathy in mice: sequence of histologic and immunohistochemical events. *Kidney Int*. 2000;58(4):1797–1804.
36. Weening JJ, Van Guldener C, Daha MR, Klar N, van der Wal A, Prins FA. The pathophysiology of protein-overload proteinuria. *Am J Pathol*. 1987;129(1):64–73.
37. Morita H, et al. Heparan sulfate of perlecan is involved in glomerular filtration. *J Am Soc Nephrol*. 2005; 16(6):1703–1710.
38. Reiser J, et al. Induction of B7-1 in podocytes is associated with nephrotic syndrome. *J Clin Invest*. 2004; 113(10):1390–1397.
39. D'Agati VD. Podocyte injury in focal segmental glomerulosclerosis: Lessons from animal models (a play in five acts). *Kidney Int*. 2008;73(4):399–406.
40. Kerjaschki D. Dysfunctions of cell biological mechanisms of visceral epithelial cell (podocytes) in glomerular diseases. *Kidney Int*. 1994;45(2):300–313.
41. Anderson S, Brenner BM. The aging kidney: structure, function, mechanisms, and therapeutic implications. *J Am Geriatr Soc*. 1987;35(6):590–593.
42. Kaplan C, Pasternack B, Shah H, Gallo G. Age-related incidence of sclerotic glomeruli in human kidneys. *Am J Pathol*. 1975;80(2):227–234.
43. McCray BA, Taylor JP. The role of autophagy in age-related neurodegeneration. *Neurosignals*. 2008; 16(1):75–84.
44. Pandey UB, et al. HDAC6 rescues neurodegeneration and provides an essential link between autophagy and the UPS. *Nature*. 2007;447(7146):859–863.
45. Lamark T, Johansen T. Autophagy: links with the proteasome [published online ahead of print December 2, 2009]. *Curr Opin Cell Biol*. doi:10.1016/j.ceb.2009.11.002.
46. Korolchuk VI, Mansilla A, Menzies FM, Rubinsztein DC. Autophagy inhibition compromises degradation of ubiquitin-proteasome pathway substrates. *Mol Cell*. 2009;33(4):517–527.
47. Rubinsztein DC, Gestwicki JE, Murphy LO, Klionsky DJ. Potential therapeutic applications of autophagy. *Nat Rev Drug Discov*. 2007;6(4):304–312.
48. Ishola DA Jr, et al. In mice, proteinuria and renal inflammatory responses to albumin overload are strain-dependent. *Nephrol Dial Transplant*. 2006; 21(3):591–597.
49. Eremina V, et al. VEGF inhibition and renal thrombotic microangiopathy. *N Engl J Med*. 2008; 358(11):1129–1136.
50. Neubert K, et al. The proteasome inhibitor bortezomib depletes plasma cells and protects mice with lupus-like disease from nephritis. *Nat Med*. 2008; 14(7):748–755.
51. Nyengaard JR, Bendtsen TF. A practical method to count the number of glomeruli in the kidney as exemplified in various animal species. *Acta Stereol*. 1990; 9(Pt 2):243–258.
52. Horvat R, Hovorka A, Dekan G, Poczewski H, Kerjaschki D. Endothelial cell membranes contain podocalyxin--the major sialoprotein of visceral glomerular epithelial cells. *J Cell Biol*. 1986;102(2):484–491.
53. Takemoto M, et al. A new method for large scale isolation of kidney glomeruli from mice. *Am J Pathol*. 2002;161(3):799–805.
54. Hartleben B, et al. Neph-Nephrin proteins bind the Par3-Par6-atypical protein kinase C (aPKC) complex to regulate podocyte cell polarity. *J Biol Chem*. 2008;283(34):23033–23038.
55. Lindenmeyer MT, et al. Proteinuria and hyperglycemia induce endoplasmic reticulum stress. *J Am Soc*

*Nephrol.* 2008;19(11):2225–2236.

56. Saleem MA, et al. A conditionally immortalized human podocyte cell line demonstrating nephrin and podocin expression. *J Am Soc Nephrol.* 2002; 13(3):630–638.

57. Mundel P, et al. Rearrangements of the cytoskeleton and cell contacts induce process formation during differentiation of conditionally immortalized mouse podocyte cell lines. *Exp Cell Res.* 1997;236(1):248–258.

58. Kabeya Y, et al. LC3, a mammalian homologue of yeast Apg8p, is localized in autophagosome membranes after processing. *EMBO J.* 2000; 19(21):5720–5728.

59. Huber TB, et al. Podocin and MEC-2 bind cholesterol to regulate the activity of associated ion channels. *Proc Natl Acad Sci U S A.* 2006;103(46):17079–17086.

60. Huber TB, et al. Nephrin and CD2AP associate with phosphoinositide 3-OH kinase and stimulate AKT-dependent signaling. *Mol Cell Biol.* 2003;23(14):4917–4928.

61. Shih NY, et al. Congenital nephrotic syndrome in mice lacking CD2-associated protein. *Science.* 1999;286(5438):312–315.